Modeling of Pulse Transformers with Parallel- and Non-Parallel-Plate Windings for Power Modulators

J. Biela, D. Bortis and J.W. Kolar
Power Electronics Laboratory, ETH Zurich
Physikstrasse 3
CH-8092, Zurich, Switzerland

ABSTRACT

The parasitic capacitances of transformers significantly influence the resulting pulse shape of a power modulator system. In order to predict the pulse shape and optimize the geometry of the pulse transformer before building the transformer an equivalent circuit and analytic expressions relating the geometry with the parasitic elements are needed. Therefore, a model consisting of 6 equivalent capacitors and a simplified circuit as well as the belonging equations are presented in this paper. The equations are verified by measurement results for pulse transformers with parallel- and non parallel-plate windings and a solid state modulator designed for linear accelerators.

Index Terms — **Pulse power systems, Pulse transformers, Pulse shaping methods, Transformer modeling, Parasitic capacitance**

1 INTRODUCTION

High voltage and high power pulses are used in a wide variety of applications, for example in accelerators, radar, medical radiation production or ionization systems. In many of these applications the requirements on the generated pulses regarding for example rise/fall time, overshoot, pulse flatness and pulse energy are high. The pulses for these applications are usually generated with pulse modulators, which often use a pulse transformer for generating high output voltages. There, the parasitic elements of the transformer significantly influence the achievable shape of the pulse.

For predicting the pulse shape of the modulator system, for designing pulse forming networks and for optimizing the geometry of the pulse transformer before building it an appropriate equivalent circuit of the transformer is needed. This equivalent circuit must on the one hand predict the transfer function of the transformer and on the other hand the parameters of the circuit should be analytically calculable with the geometric and electric parameters of the transformer. Therefore, an equivalent model of the pulse transformer and the analytic equations for calculating the parameters are presented in this paper.

In [1, 2] a simple L-L-C model of the transformer is used to predict the resulting pulse shape. The value of the capacitance in this model is calculated by applying the equation for parallel-plate capacitor [1] and for non parallel-plate capacitor [2] on the primary / secondary winding interface what results in

$$C_{\backslash /} = \frac{\varepsilon\, l_{Wdg} h_{Wdg}}{d_{Wdg}} \left(\frac{N-1}{N} \right)^2 \Bigg| C_{||} = \frac{\varepsilon\, l_{Wdg} h_{Wdg}}{d_{Wdg}} \left(\frac{N^2+N+1}{N^2} \right). \qquad (1)$$

In both, only the distributed electric energy in the volume directly between the primary and the secondary winding is considered, what results in a relatively poor accuracy. This could be seen in figure 1 where a measured and two calculated pulse responses of a transformer are shown. The input voltage of the calculation models was the measured output voltage of the solid state switch. In contrast to the prediction of the simple models the result of the extended model matches the measurement results much better. In this model all the regions which are relevant with respect to the distributed energy are considered.

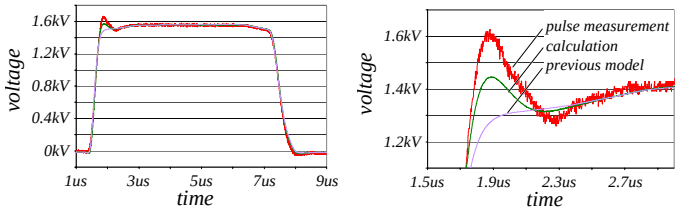

Figure 1. Comparison of measurement and the two different calculations

Thus, in section II of this paper first the energies which are stored in the different relevant regions are calculated by analytic approximations. In the next step the calculated energies are compared with the energies stored in the equivalent circuit in section III. By this comparison the parameters of the equivalent circuit of the pulse transformer are determined. The suggested model comprises six capacitors and could be used in any connection of the transformer. If both windings are grounded the model could be simplified to an equivalent circuit with just one capacitor. With the considerations of section II the capacitances of the equivalent network can be calculated by means of the transformer geometry. Based on this equation a good prediction of the pulse shape is possible as shown in figure 1.

Another possibility to obtain the parameter of the suggested

equivalent circuit is to use 2D FEM-simulations. For this reason the setup of the simulations is explained in section IV. The described setups also could be used to parameterize the model by impedance measurements.

In section V the proposed equations are validated by comparing the calculated and the measured pulse shape for different operation and load conditions for a solid state pulse modulator. Finally, a conclusion is presented in section VI.

2 CALCULATION OF PARASITIC CAPACITANCES

For determining the equivalent capacitances of the pulse transformer's equivalent circuit the distributed energies in all regions must be calculated. In order to be able to calculate the stored energies the 3 dimensional distribution of the electric field strength must be known. The field distribution, however, generally only could be calculated with time consuming numeric FEM-simulations.

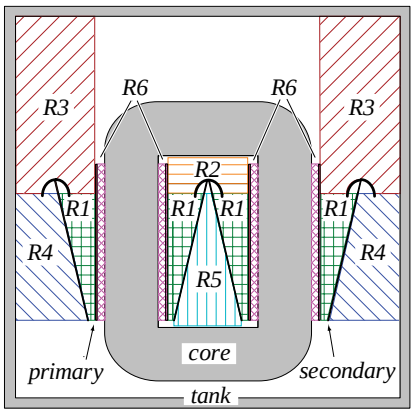

Figure 2. Regions for the distributed capacitance of a pulse transformer with non parallel-plate windings.

Since in most regions the run of the electric flux lines approximately lies within a plane which is parallel to the winding axis, the per unit energies for these planes are considered in the following. In figure 2 a 2D cut of the transformer with surrounding tank is given. There, six different planes/regions are shown which are considered in the following for calculating the stored energy.

Since the calculations are performed for planes per unit energies result. In order to obtain the value of the stored energy of the respective region the per unit energy must be multiplied by the lengths shown in figure 3.

The areas/volumes which are not covered by a region are neglected in the following, since the energy density and therewith the share in the total equivalent capacitance is relatively small as could be proven by FEM-simulations.

The presented calculations are performed for pulse transformers with non parallel-plate and also for transformers with parallel-plate windings. However, the presented procedure can analogically applied to other winding arrangements. Furthermore, it is assumed that the core and also the tank is grounded what is usually true in practice.

In the following paragraphs the stored energies for the six

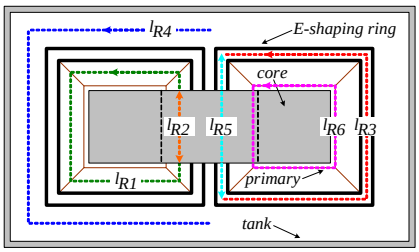

Figure 3. Definition of the lengths for the distributed capacitances.

regions are calculated separately. There, the presented equations always represent the part of the energy which is stored in the winding of one leg, that means that for example the energies must be multiplied by two for the setup shown in figure 2/3.

2.1 ENERGY BETWEEN THE WINDINGS – R_1

In region R_1 the area between the primary and the secondary winding is summarized. This is the only area which is considered for determining the equivalent circuit of the pulse transformer in the approach presented in [1, 2] – cf. equation (1).

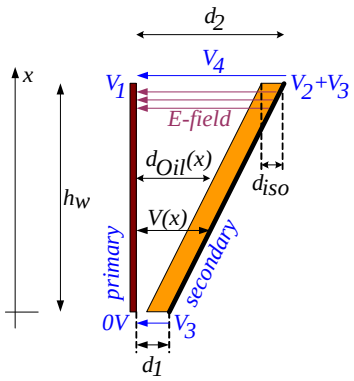

Figure 4. Calculation of the energy W_{R1} by means of the parallel plate capacitor equations.

For simplifying the calculation of the energy W_{R1} between the primary and the secondary it is assumed in the following that both windings approximately could be modeled by a conductive plate with a linear voltage distribution. The primary winding is grounded at the lower side and the voltage at the upper end is V_1, whereas the voltage distribution of the secondary winding starts at the offset voltage V_3 at the lower end and ends at V_2+V_3 as shown in figure 4. In case the secondary winding is also grounded voltage V_3 is zero.

With the assumed voltage distribution the voltage difference between the two plates and the distance between the two plates could be written as

$$V(x)=\frac{x}{h_W}(V_4-V_3)+V_3 \quad \Big| \quad d(x)=d_{Oil}(x)+d_{Iso}=\frac{d_2-d_1}{h_W}x+d_1 \,. \quad (2)$$

There, d_1 is the distance at the lower end and d_2 at the upper end.

In order to simplify the calculations further, the electric flux lines between the primary and the secondary winding in region R_1 are approximated by straight lines which are orthogonal to the primary winding. In this case the energy stored in the differential element dx could be calculated by

$$dW'_{R1}=\frac{\varepsilon V^2(x)}{2\left(d_{Oil}(x)+d_{Iso}\right)}dx=\frac{\varepsilon}{2}\frac{\left((V_4-V_3)x+V_3h_W\right)^2}{\left((d_2-d_1)x+d_1h_W\right)h_W}dx \,. \quad (3)$$

Integrating this expression along the primary winding yields the total per unit energy W'_{R1} which is stored in the plane (R_1) between the two plates. Multiplying the per unit energy by the

length l_{R1} (cf. fig. 3) yields the energy W_{R1} stored in region R_1.

$$W_{R1} = l_{R1} \int_0^{h_W} \frac{\varepsilon}{2} \frac{\left((V_4 - V_3)x + V_3 h_W\right)^2}{\left((d_2 - d_1)x + d_1 h_W\right) h_W} dx \,. \quad (4)$$

In general, this energy depends on the voltage difference between the two plates and also on the offset voltage of the secondary winding. The evaluated integral is given in the appendix.

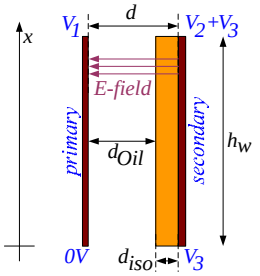

Figure 5. Calculation of the energy W_{R1} for parallel plate windings.

So far it has been assumed that the materials between the two plates have the same permittivity $\varepsilon_{Iso} = \varepsilon_{Oil} = \varepsilon = \varepsilon_0\varepsilon_R$. Usually, the space between the two windings is filled with oil and the coil former of the secondary winding. If these two materials have a different permittivity an equivalent value for the permittivity could be calculated by

$$\varepsilon_{eq}(x) = \frac{\varepsilon_{Iso} \cdot \varepsilon_{Oil} \cdot \left(d_{Iso} + d_{Oil}(x)\right)}{\varepsilon_{Iso} \cdot d_{Oil}(x) + \varepsilon_{Oil} \cdot d_{Iso}} \,. \quad (5)$$

This equivalent permittivity is a function of x since the path length of the field line in the oil varies with x. Substituting the permittivity in equation (3) by this expression and calculating the energy results in (cf. appendix)

$$W_{R1} = \frac{1}{2} \int_0^{h_W} \frac{l_{R1}\, \varepsilon_{Iso}\, \varepsilon_{Oil} \left((V_4 - V_3)x + V_3 h_W\right)^2 dx}{\left(\varepsilon_{Iso}\left[(d_2 - d_1)x + (d_1 - d_{Iso})h_W\right] + \varepsilon_{Oil}\, d_{Iso} h_W\right) h_W} \,. \quad (6)$$

Again, the voltage V_3 could be set to zero if the secondary windings is also grounded and the voltage V_4 could be substituted by $V_4 = V_2 - V_1$.

For a transformer with parallel windings the distance d is constant (cf. eq. (2) and figure 5) and the energy in region R_1 is

$$W_{R1,\parallel} = \frac{1}{2} \int_0^{h_W} \frac{\varepsilon_o \varepsilon_{iso} \varepsilon_{Oil} \left((V_2 - V_1)x/h_W + V_3\right)^2}{\left(\varepsilon_{iso} d_{Oil} + \varepsilon_{Oil} d_{iso}\right)} dx = \frac{\varepsilon_o \varepsilon_{iso} \varepsilon_{Oil}}{\left(\varepsilon_{iso} d_{Oil} + \varepsilon_{Oil} d_{iso}\right)} \left(\frac{\left(V_2 - V_1 + V_3\right)^3 - V_3^3}{6\left(V_2 - V_1\right)} \right) h_W \,. \quad (7)$$

2.2 WINDING WINDOW: ABOVE SECONDARY – R_2

Region R_2 consists of the area above the secondary winding within the winding window. The border of this region has a complex shape which is determined by the core, the primary winding and the E-field shaping ring. In order to be able to calculate the distributed capacitance of this region analytically the geometry is simplified as shown in figure 6. First, it is assumed that the primary winding consists of a metal plate which is grounded, i.e. V_1 is neglected since $V_2 = N \cdot V_1 >> V_1$. Furthermore, this plate is extended so that the upper end touches the core. Second, the influence of the secondary winding is neglected as well as the E-field shaping ring and the core/extended primary are replaced by circles. These simplifications result in a coaxial structure whose energy is approximately (±10%) the same as the one of the original structure as has been proven by FEM-simulations.

The energy stored in the coaxial structure in figure 7(a) could

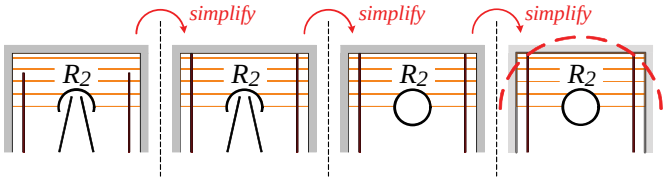

Figure 6. Simplification of the region R_2 to a coaxial structure.

be calculated with the equation for the cylindrical capacitor, what results in the per unit equation

$$W'_{R2} = \frac{1}{4} \frac{\pi \varepsilon_{Oil}}{\ln\left(r_o / r_i\right)} \left(V_2 + V_3\right)^2 = \frac{\pi \varepsilon_{Oil} \left(V_2 + V_3\right)^2}{4 \ln\left(k\, d / r_i\right)} \quad \text{with} \quad k = 1.08. \quad (8)$$

There, only one half of the energy is calculated since equation (8) represents the part of the energy which is stored in the winding of one leg. i.e. half the region R_2.

The factor k is empirically determined by FEM-simulations so that the resulting difference between the energy of the original structure and the equivalent one is minimal. In [3] a similar transformation is described but the factor k is set equal to 1.16. For the considered setup, this choice resulted in a larger error for the equivalent energy than k=1.08.

In order to obtain the energy W_{R2} the per unit energy W'_{R2} must be multiplied by l_{R2}. This energy is independent of the winding arrangement (parallel- or non-parallel-plate).

2.3 ABOVE SECONDARY WINDING OUTSIDE WINDING WINDOW – R_3

Region R_3 is the equivalent of region R_2 outside the winding window, but there the run of the border in the upper region is more complex. For simplifying the setup it is assumed that the primary winding consists of a grounded plate (i.e. neglect $V_1 << V_2$) which is stretched to the cover of the tank. The influence of the cover itself is neglected since its distance to the E-field shaping ring is relatively large (cf. fig. 2). Furthermore, it is assumed that the E-field shaping ring is in the middle of the primary winding and the wall of the tank, what is approximately fulfilled for a compact design, where the distance between the E-field shaping ring and the tank is equal to the minimum possible one fixed by the insulation requirements.

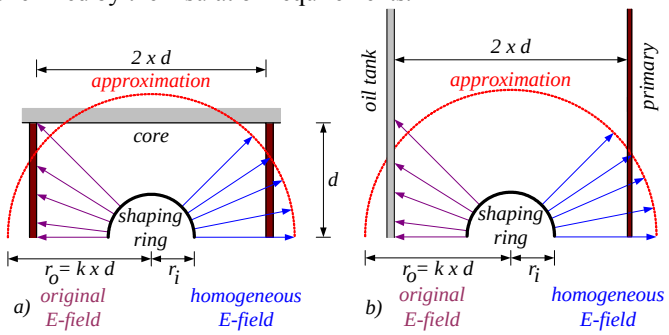

Figure 7. (a) Equivalent structure for calculating the energy of region R_2. (b) Original and simplified geometry for region R_3.

The resulting rectangular border is again approximated by a coaxial structure as shown in figure 7(b). With this approximation the stored energy for this structure could be calculated by

$$W_{R3} = \frac{l_{R3}}{2}\frac{\pi\,\varepsilon_{Oil}}{\ln\left(k\,d/r_i\right)}\left(V_2+V_3\right)^2 \text{ with } k=1.275, \qquad (9)$$

where k is empirically adapted by FEM-simulations again. For this structure the value which results in a minimum error is 1.275, which is the same as proposed in [2].

Remark: In case the transformer is not inside a grounded tank the plate on the left hand side in figure 7(b) must be omitted. There, the geometry could be simplified by assuming that the primary winding is grounded and extended to infinity so that the energy in this region could be calculated with the equations for the capacitance of two wire line (transmission line). This results in

$$W_{R3,II} = l_{R3}\frac{\pi\,\varepsilon_{Oil}}{\ln\left(2d/r_i+\sqrt{\left(2d/r_i\right)^2-1}\right)} \qquad (10)$$

for the energy stored in region R_3 which is again independent of the winding arrangement.

2.4 BETWEEN SECONDARY AND TANK – R_4

The energy between the secondary and the wall of the tank below the E-field shaping ring is partially included in region R_4. There, the wall of the tank and the secondary winding form a non-parallel plate capacitor with a approximately linear voltage distribution again. The voltage and the distance between the plates are given as a function of x by

$$V(x)=\frac{x}{h_w}V_2+V_3 \quad \Big| \quad d(x)=\frac{d_2'-d_1'}{h_w}x+d_1', \qquad (11)$$

where the variables are defined as shown in figure 8(a). Using these expressions the energy could be calculated by

$$W_{R4} = l_{R4}\int_0^{h_w}\frac{\varepsilon_{Oil}}{2}\frac{\left(V_2\,x+V_3\,h_w\right)^2}{\left(\left(d_2'-d_1'\right)x+d_1'\,h_w\right)h_w}dx \qquad (12)$$

as described in section II.A (cf. appendix). For a transformer with parallel windings the wall of the tank and the secondary winding form a parallel plate capacitor and equation (12) could be simplified to

$$W_{R4,||} = \frac{1}{2}\int_0^{h_w}\frac{\varepsilon_0\varepsilon_{oil}\left(V_2/h_w\,x+V_3\right)^2}{d_2'}dx = \frac{\varepsilon_0\varepsilon_{oil}}{d_2'}\frac{V_2^2+V_2V_3+V_3^2}{6}h_w \qquad (13)$$

since the distance d (cf. eq. (11)) is constant.

Assuming a compact system, the distances could be set to $d'_2 = d_2$ and $d'_1 = 2d_2 - d_1$ as also has been done for region R_3.In figure 8(b) a plot of the simulated electric flux lines between the secondary winding and the tank is shown. There, it could be seen that especially at the upper and the lower end of the winding (blue circles) the run of the simulated flux lines deviates from the one which has been assumed in the calculation model for region R_4. At the upper end the reason for the deviation is the E-field shaping ring. At the lower end the field is mainly distorted by the voltage distribution on the secondary and also by the proximity of the core and the primary winding. With a parallel winding arrangement the distortion at the lower end is much smaller than with a non parallel-plate winding as shown in figure 8(d).

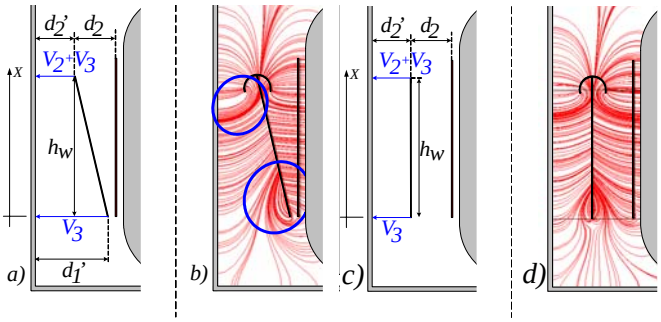

Figure 8. Definition of the variables for region R_4 for non-parallel plate (a) and parallel plate windings (c). Electric flux lines between the secondary winding and the wall of the tank for non parallel plate (b) and parallel plate windings (d).

These deviations result in a reduced accuracy of the explained calculation method for region R_4. The exact run of the flux lines, however, just could be calculated with time consuming FEM-simulations. Furthermore, due to the small share of the energy stored in these parts of region R_4 in the overall stored energy the resulting overall error for calculating the effective capacitance is relatively small.

Remark: In case the transformer is not inside a grounded tank the deviations at the lower end of the secondary winding shown in the blue circle in figure 8(b) increase. That means that the electric flux lines at the left side of the secondary winding in figure 8(b) tend to start at the upper end of the winding and end at the lower end/core. Unfortunately, the energy stored within this field distribution could not be easily calculated with the approaches used here. Instead of that the energy must be calculated by FEM-simulations.

2.5 WINDING WINDOW: BELOW SECONDARY – R_5

In the next step the energy stored in region R_5, i.e. below the secondary winding in the winding window, is calculated. There, the electric flux lines are approximated by straight lines again. These lines start at the secondary winding and are orthogonal to the winding window of the grounded core as shown in figure 9(a).

With this approximation the stored energy could be calculated as described in section II.A for region R_1. The resulting equations are

$$V(x)=\frac{x}{d_2-d_1}V_2+V_3 \quad \Big| \quad d(x)=\frac{h_w}{d_2-d_1}x+d_0 \qquad (14)$$

and

$$W_{R5} = l_{R5}\int_0^{d_2-d_1}\frac{\varepsilon_{Oil}\left(\left(d_2-d_1\right)V_3+V_2\,x\right)^2}{2\left(d_2-d_1\right)\left(d_0\left(d_2-d_1\right)+h_w x\right)}dx \qquad (15)$$

where the evaluated integral is given in the appendix again.
Due to the limited volume and the low average energy density the stored energy usually is relatively small and could be neglected in many cases. This is particularly true for parallel-plate windings which can not be modeled by simple analytical approaches why the equations are omitted.

2.6 AREA BETWEEN PRIMARY AND CORE - R_6

Finally, the energy stored between the primary winding and the core is calculated which is independent of the winding arrangement. The structure of the winding and the core act like a parallel plate capacitor with two different dielectrics – the oil and

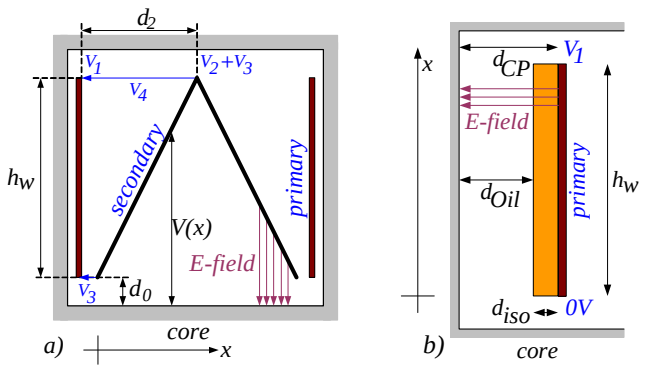

Figure 9. (a) Variables / simplified run of electric flux lines for region R_5. (b) Definition of variables for region R_6.

the coil former of the primary winding as shown in figure 9(b). Assuming a linear voltage distribution again, the voltage distribution, the distance and the permittivity are

$$V(x) = \frac{x}{h_W} V_1 \quad \Big| \quad d(x) = d_{Oil,P} + d_{Iso,P}$$
$$\varepsilon_{eq} = \frac{\varepsilon_{Iso}\varepsilon_{Oil}(d_{Iso,P} + d_{Oil,P})}{\varepsilon_{Iso} d_{Oil,P} + \varepsilon_{Oil} d_{Iso,P}} \tag{16}$$

and the energy could be calculated by

$$W_{R6} = \frac{1}{6} \frac{\varepsilon_{Iso}\varepsilon_{Oil}(d_{Iso,P} + d_{Oil,P}) h_W}{\left(\varepsilon_{Iso} d_{Oil,P} + \varepsilon_{Oil} d_{Iso,P}\right) d_{CP}} V_1^2 \, l_{R6} \,. \tag{17}$$

2.7 WINDING CAPACITANCE

So far, only the stored energy/capacitances between the windings or between one winding and the core/tank have been considered. But also between the singe turns of one winding electric energy is stored. This energy could be calculated by approaches presented in [5-7].

Due to fact that the windings are usually implemented with only one / two layers and the turn to turn voltage is relatively small as well as the distance between the single turns is relatively large due to the insulation this part of the stored energy usually could be neglected.

3 EQUIVALENT CIRCUIT OF A PULSE TRANSFORMER

In the last preceding section the energies stored in the different regions of the pulse transformer/tank setup have been calculated. In the next step the parameters of the equivalent circuit of this setup are calculated. This is performed by comparing the energy stored in the equivalent circuit, which is a function of the independent voltages V_1-V_3, with the calculated stored energy, which is also a function of V_1-V_3 (V_4=V_2+V_3-V_1). For determining the energy stored in the equivalent circuit, first an appropriate equivalent circuit must be chosen.

As could be shown the electrostatic behavior of an arbitrary transformer could be modeled by a three input multipole (primary and secondary voltage and the voltage between the windings) [3]. In the linear working area and as long as propagation times can be ignored, the electrostatic energy / behavior of this multipole could be modeled by six independent capacitors as shown in figure 10.

The energy stored in the equivalent circuit is given by

$$W_{Eq} = \frac{1}{2}\begin{pmatrix} C_1 V_1^2 + C_2 V_2^2 + C_3 V_3^2 + C_4 (V_2 + V_3 - V_1)^2 \\ + C_5 (V_2 + V_3)^2 + C_6 (V_1 - V_3)^2 \end{pmatrix} \tag{18}$$

what results from $1/2 C V_C^2$. In the same manner the calculated energy stored in the different regions of the setup in figure 2 could be written

$$W_{Cal} = 2\left(W_{R1} + W_{R2} + W_{R3} + W_{R4} + W_{R5} + W_{R6}\right) = f(V_1, V_2, V_3), \tag{19}$$

where V_4 has been replaced by $V_4 = V_2$+V_3-V_1 and the factor 2 results from the fact that the energies have been calculated for each leg separately.

Since both energies must be equal W_{Eq}=W_{Cal} the equations of the capacitors can be derived by setting the coefficients of the variables/voltage terms V_1, V_2, V_3, V_1V_2, V_1V_3 and V_2V_3 equal. This results in six independent equations which can be solved for the capacitances C_1-C_6.

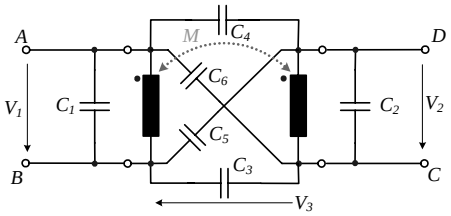

Figure 10. General equivalent circuit of pulse transformer.

In contrast to the results published in [3] the capacitors C_1/C_2, C_3/C_4 and C_5/C_6 are not interdependent for the non parallel-plate winding since the windings are not arranged in parallel and therefore the winding construction is not symmetric with respect to the low and the high side.

With the described model the transfer behavior of the pulse transformer and therewith the influence on the transferred pulse shape could be calculated and/or simulated for arbitrary connections. Moreover, with the equations relating the geometry of the transformer directly with the capacitances of the equivalent model the construction of the transformer could be optimized for the required transfer behavior.

3.1 SIMPLIFIED CIRCUIT WITH NEW EQUATIONS

In many pulse power applications the pulse transformer is not used for galvanic isolation and the low side of the primary as well as the low side of the secondary winding are grounded, i.e. $V_3 = 0$ in figure 10. In this case capacitor C_3 is replaced by a short circuit and C_1/C_6 as well as C_2/C_5 are in parallel. Moreover, the voltages across all capacitors could be derived from the primary and/or secondary voltage by using the turns ratio N. With the voltages known the energy which is stored in the capacitors could be calculated as a function of the secondary (or primary) voltage.

$$W = \frac{C_1 + C_6 + C_4 (N-1)^2 + (C_2 + C_5) N^2}{2} V_2^2 = \frac{C_d}{2} V_2^2 \tag{20}$$

Furthermore, the equivalent circuit could be simplified to the circuit shown in figure 11(a). Neglecting the parallel resonance between the leakage and capacitor C_4 this circuit could be further

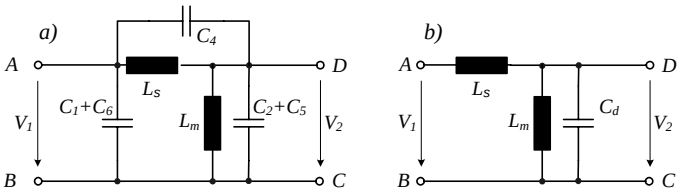

Figure 11. (a) Simplified equivalent circuit (cf. fig.10). (b) Approximated simplified circuit with capacitances transferred to secondary side.

simplified to the circuit shown in figure 11(b), where only one capacitor is used which is transferred to the secondary side.

The capacitance value for the equivalent capacitor referred to the secondary side is

$$C_d = \frac{C_1 + C_6}{N^2} + \frac{C_4 (N-1)^2}{N^2} + (C_2 + C_5) \qquad (21)$$
$$\Rightarrow C_d \sim C_2 + C_4 + C_5 \quad \text{for large } N$$

The circuit of figure 11(b) is the same as used in [1, 2] but in those publications no equation for calculating the equivalent capacitance C_d from the geometry of the transformer was given except for the simple parallel plate approach for the region between the windings.

4 DETERMINATION OF THE EQUIVALENT CIRCUIT BY FEM-SIMULATION OR MEASUREMENT

Besides the presented possibility to calculate the values of the six capacitors of the general equivalent circuit (cf. fig. 9) by means of the transformer geometry it is also possible to obtain the values by measurement or by FEM-simulation.

Since there are six independent capacitors in the equivalent circuit, six independent simulations / measurements must be carried out. The belonging measurement setups are shown in figure 12.

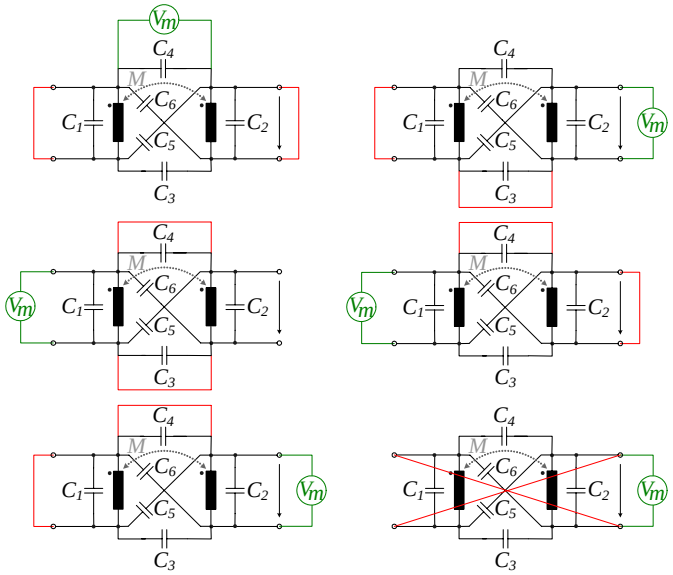

Figure 12. Measurements for determining the equivalent capacitances.

For the measurement results following below the values of the capacitances have been determined by using resonance peaks in the impedance plot. The required inductance values are directly

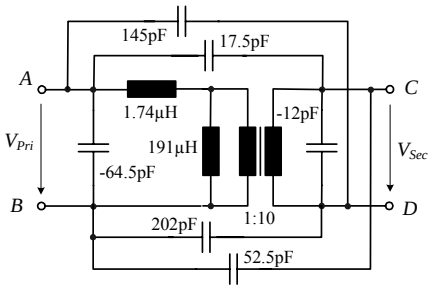

Figure 13. Calculated equivalent circuit for the transformer in figure 14(b).

measured with an impedance analyzer Agilent 4294A and then the capacitances are calculated with the frequency of the resonance peak.

$$C_1 = \frac{1}{2}(C_{M2} - C_{M3} - C_{M4} + C_{M6}) \quad C_2 = \frac{1}{2}(-C_{M1} + C_{M3} + C_{M4})$$
$$C_3 = \frac{1}{2}(-C_{M2} + C_{M3} + C_{M5}) \quad C_4 = \frac{1}{2}(C_{M1} - C_{M3} - C_{M5} + C_{M6}) \qquad (22)$$
$$C_5 = \frac{1}{2}(C_{M4} + C_{M5} - C_{M6}) \quad C_6 = \frac{1}{2}(C_{M1} + C_{M2} - C_{M4} - C_{M5})$$

With the measured capacitances the values of the equivalent capacitors of the circuit in figure 10 could be calculated by the following equations (cf. figure 13).

Instead of measuring the capacitances with an impedance analyzer, the same setups could be used for determining the capacitances by FEM-simulations. There, either 3D simulations, which are quite accurate but very time consuming, or 2D simulations as shown in figure 14, which are much faster but less accurate, could be performed. The equivalent capacitors could be calculated with the same equations (22) as used for the measurements.

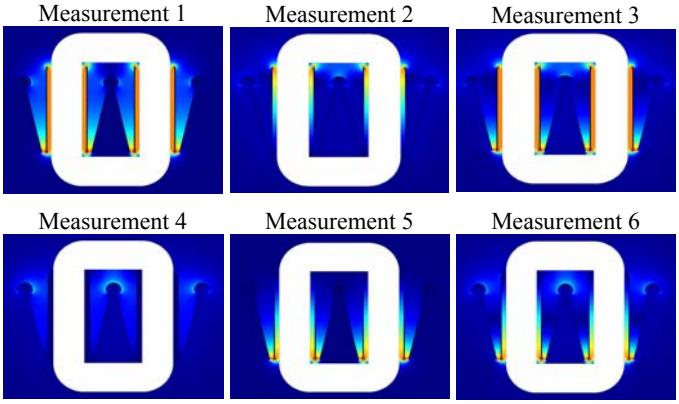

Figure 14. 2D FEM-simulations for a transformer with non parallel-plate windings (cf. figure 15(b)).

5 MEASUREMENT RESULTS

In order to verify the presented equations measurements at the pulse transformers shown in figure 15 excited by the solid state modulator shown in figure 16 have been carried out. The measurements have been conducted at relatively low voltage (<2kV) so that very fast and accurate probes could be used and measurement errors related to voltage dividers could be minimized. Furthermore, during the measurements both windings were grounded, i.e. $V_3 = 0$, and the transformer was not

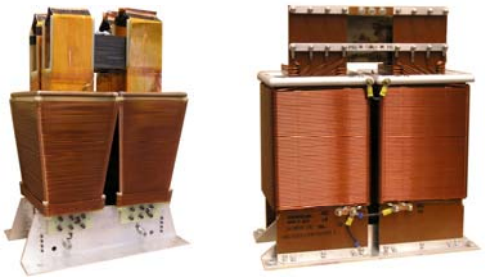

Figure 15. Picture of the pulse transformer with non parallel-plate (a) and parallel-plate windings (b) used for the measurements.

inside a tank since none was available at the time of measurement. Further measurement results with tank and also loss equations will be presented in a future paper.

The equivalent circuit calculated for the transformer shown in figure 15 is given in figure 13. There, also the leakage inductance and the magnetizing inductance are shown, which can be calculated from the magnetic field distribution in the window / core.

In table 1 measurement, simulation and calculation results for the transformers shown in figure 15 are given. There, it could be seen that the analytic and simulated values correspond very well with the measured ones.

Table 1 - Values for C_{M1} - C_{M6} for measurements, simulation and analytic calculation for the transformers shown in figure 15 with non-parallel-plates (a) and parallel plates (b) in air without tank.

a)	Measured	Simulated	Calculated
1	1.19 nF	1.15 nF	1.25 nF
2	350 pF	320 pF	316 pF
3	1.2 nF	1.1 nF	1.25 nF
4	50 pF	63 pF	50 pF
5	347 pF	450 pF	350 pF
6	325 pF	427 pF	360 pF

b)	Measured	Simulated	Calculated
1	418 pF	446 pF	428 pF
2	121 pF	138 pF	127 pF
3	335 pF	394 pF	393 pF
4	58 pF	53pF	49 pF
5	190 pF	167 pF	141 pF
6	150 pF	133 pF	153 pF

In figure 17 for example measured pulse responses and in figure 18 the overshoot in an enlarged scale are shown for a solid state modulator with the specification given in table 2 and a transformer with parallel-plate windings. Additionally, curves

Figure 16. Solid state modulator with 4kA/1kV per switch used for measurements.

resulting from the model with six capacitors where the capacitance values have been determined by analytic calculations, simulations and impedance measurements are shown in figure 18. There, it could be seen that the pulse shape including ringing could be predicted very well by means of the presented set of new equations.

Table 2 - Specification of solid state modulator

Output voltage	200kV
Output Power	20MW
Pulse Duration	3-7µs
Repetition rate	500Hz

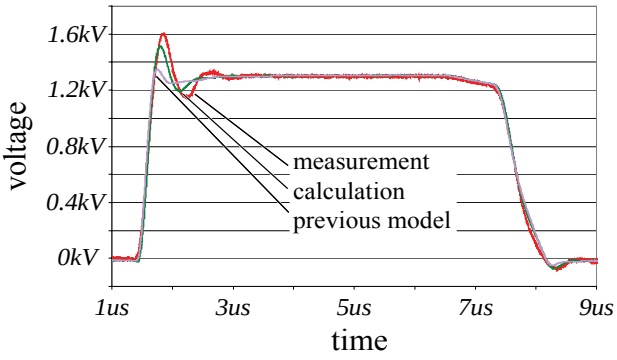

Figure 17. Measured and calculated pulse response for a load resistance of 2500Ω and the transformer with parallel-plate windings.

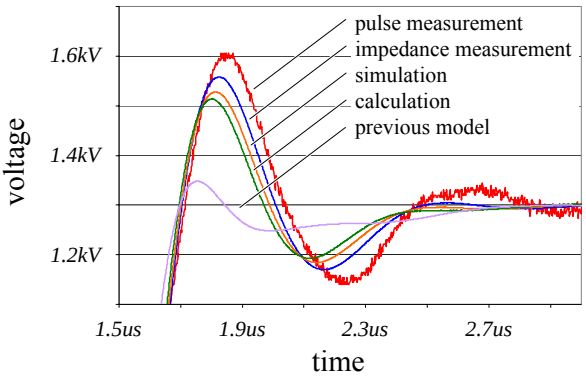

Figure 18. Measured, simulated and calculated pulse for 2500Ohm load.

6 CONCLUSION

In this paper a general model for pulse transformers which allows for predicting the pulse shape of a modulator system before building the transformer is presented. The parameters of the model can be calculated analytically from the geometry of the transformer or can be determined by simulation or measurement.

If both windings are connected to ground the presented model could be simplified to the known L-L-C. Furthermore, from the equations of the general model, new analytic expressions for determining the parameters of the simple model based on the energy distribution in all relevant regions of the transformer are derived.

Both, the general and the simplified model based on the new

equations show a good correspondence with the presented measurement results for non parallel-plate and also for parallel plate winding arrangements.

APPENDIX - EQUATIONS

In the following the evaluated integral equations for the regions R_1, R_4 and R_5 are listed.

In region R_1 the energy for $\varepsilon_{Iso} = \varepsilon_{Oil} = \varepsilon$, i.e. eq. (4), could be calculated by

$$W_{R1} = \frac{l_{R1}\,\varepsilon\,h_W}{4\left(d_1 - d_2\right)^3}\begin{bmatrix} 2\left(d_1V_4 - d_2V_3\right)^2\left(\ln d_1 - \ln d_2\right) + \\ +\left(V_3 - V_4\right)\left(d_1 - d_2\right)\cdot \\ \cdot\left(\left(V_3 + 3V_4\right)d_1 - \left(V_4 + 3V_3\right)d_2\right) \end{bmatrix} \quad (23)$$

and for unequal permittivities by

$$W_{R1} = \frac{l_{R1}\,\varepsilon\,h_W}{4\left(d_1 - d_2\right)^3}\begin{bmatrix} \left(\left(\left(V_3 - V_4\right)d_{Iso} - V_3d_2 + V_4d_1\right)\cdot\right)^2 \\ \varepsilon_{Iso} + \left(V_4 - V_3\right)d_{Iso}\varepsilon_{Oil} \\ \left(\ln\left(\left(d_1 - d_{Iso}\right)\varepsilon_{Iso} + d_{Iso}\varepsilon_{Oil}\right) - \right) \\ \left(-\ln\left(\left(d_2 - d_{Iso}\right)\varepsilon_{Iso} + d_{Iso}\varepsilon_{Oil}\right)\right) + \\ +\tfrac{1}{3}\left(V_4 - V_3\right)\left(d_2 - d_1\right)\cdot \\ \left(\begin{pmatrix} 2\left(V_4 - V_3\right)d_{Iso} \\ +\left(d_2 - 3d_1\right)V_4 \\ +3\left(d_2 - \tfrac{1}{3}d_1\right)V_3 \end{pmatrix}\varepsilon_{Iso}\right)\varepsilon_{Iso} \\ -2\varepsilon_{Oil}d_{Iso}\left(V_4 - V_3\right) \end{bmatrix}. \quad (24)$$

The energy stored in region R_4 results with equation (12) from

$$W_{R4} = \frac{l_{R4}\,\varepsilon_{Oil}\,h_W}{2\left(d_1' - d_2'\right)^3}\begin{bmatrix} \left(\left(V_2 + V_3\right)d_1' - V_3d_2'\right)^2\left(\ln d_1' - \ln d_2'\right) \\ -\frac{3}{2}V_2\left(d_1' - d_2'\right)\cdot \\ \cdot\left(\left(V_2 + \frac{4}{3}V_3\right)d_1' - \frac{1}{3}\left(4V_3 + V_2\right)d_2'\right) \end{bmatrix}. \quad (25)$$

There, the variables d'_1 and d'_2 are defined in figure 9. Finally the energy stored in region R_5 could be calculated with

$$W_{R5} = \frac{l_{R5}\varepsilon_{Oil}\left(d_2 - d_1\right)}{2h_W^3}\begin{bmatrix} \left(V_2d_0 - V_3h_W\right)^2\left(\ln\left(d_0 + h_W\right) - \ln d_0\right) \\ +h_wV_2\left(\left(2V_3 + \frac{1}{2}V_2\right)h_W - V_2d_0\right) \end{bmatrix}. \quad (26)$$

REFERENCES

[1] N. G. Glasoe and J. V. Lebacqz, "Pulse Generators", MIT Radiation Laboratory Series, vol. 5, McGraw-Hill Book Company, New York, 1948.

[2] M. Akemoto, S. Gold, A. Krasnykh and R. Koontz, "Pulse Transformer R&D for NLC Klystron Pulse Modulator", SLAC, Stanford University.

[3] Harold A. Wheeler, "Transmission-Line Properties of a Round Wire in a Polygon Shield".

[4] B. Cogitore, J.-P. Keradec, J. Barbaroux, "The two-winding transformer: an experimental method to obtain a wide frequency range equivalent circuit", Trans-action on Instrumentation and Measurement, Vol. 43, April, 1994, pp. 364 – 371.

[5] A. Massarini, M.K. Kazimierczuk, "Modelling the Parasitic Capacitance of Inductors", 16 Capacitor and Resistor Technology Symposium 96, 1996, March 11-15, pp. 78–85.

[6] A. Massarini, M.K. Kazimierczuk, G.Gandi, "Lumped Parameter Models for Single- and Multiple-Layers Inductors ", 27th Power Electronics Specialists Conference PESC '96, Vol. 1, June 23-27, 1996, pp. 295 – 301.

[7] J. Biela and J.W.Kolar, "Using Transformer Parasitics for Resonant Converters – A Review of the Calculation of the Stray Capacitance of Transformers", Conference Record of the IEEE Industry Applications Conference, Hong Kong, Oct. 2-6, 2005.

Jürgen Biela (S'04) was born in Nuremberg, Germany, on July 12, 1974. He studied electrical engineering at the Friedrich-Alexander-Universität Erlangen. During his studies he dealt in particular with resonant DC-link inverters at the Strathclyde University, Scotland and the active control of series connected IGCTs at the Technical University of Munich, Germany. After he had received his diploma degree with honours from FAU Erlangen in October 2000, he worked on inverters with very high switching frequencies, SiC components and EMC at the research department of A&D Siemens, Germany. Since July 2002 he is Ph.D. student at the PES, ETH Zurich. His current research is focused on electromagnetic integration of passive components and modelling, design and optimisation of DC-DC converters.

Dominik Bortis (S'06) was born in Fiesch, Switzerland on December 29, 1980 He studied electrical engineering at the Swiss Federal Institute of Technology (ETH) Zurich. During his studies he majored in communication technology and automatic control engineering. In his diploma thesis he worked with the company Levitronix, where he designed and realised a galvanic isolation system for analog signals. He received his M.Sc. degree in May 2005, and he has been a Ph.D. student at the Power Electronic Systems Laboratory, ETH Zürich, since June 2005.

Johann W. Kolar (M' SM') studied industrial electronics at the University of Technology Vienna, Austria, where he also received the Ph.D. degree (summa cum laude). From 1984 to 2001 he was with the University of Technology in Vienna, where he was teaching and working in research in close collaboration with the industry in the fields of high performance drives, high frequency inverter systems for process technology and uninterruptible power supplies. He has proposed numerous novel converter topologies, e.g., the VIENNA Rectifier and the Three-Phase AC-AC Sparse Matrix Converter concept. Dr. Kolar has published over 150 scientific papers in international journals and conference proceedings and has filed more than 50 patents. He was appointed Professor and Head of the Power Electronics Systems Laboratory at the Swiss Federal Institute of Technology (ETH) Zurich on Feb. 1, 2001.

The focus of his current research is on novel AC-AC and AC-DC converter topologies with low effects on the mains for telecommunication systems, More-Electric-Aircraft applications and distributed power systems utilizing fuel cells. A further main area of research is the realization of ultra-compact intelligent converter modules employing latest power semiconductor technology (SiC) and novel concepts for cooling and EMI filtering.

Dr. Kolar is a Senior Member of the IEEE and a member of the IEEJ and of Technical Program Committees of numerous international conferences in the field (e.g. Director of the Power Quality branch of the International Conference on Power Conversion and Intelligent Motion). From 1997 through 2000 he served as an Associate Editor of the IEEE Transactions on Industrial Electronics and since 2001 as an Associate Editor of the IEEE Transactions on Power Electronics.